



Published in final edited form as:

Adv Exp Med Biol. 2013 ; 787: 215–222. doi:10.1007/978-1-4614-1590-9_24.

Maps of ITD in the Nucleus Laminaris of the Barn Owl

Catherine Carr,

Department of Biology, University of Maryland, College Park MD USA

Sahil Shah,

Department of Biology, University of Maryland, College Park MD USA

Go Ashida,

Department of Biology, University of Maryland, College Park MD USA

Thomas McColgan,

Institute for Biology II, RWTH Aachen, Aachen, Germany

Hermann Wagner,

Institute for Biology II, RWTH Aachen, Aachen, Germany

Paula Kuokkanen,

Humboldt University, Berlin, Germany

Richard Kempter, and

Humboldt University, Berlin, Germany

Christine Köppl

Institute for Biology and Environmental Sciences, and Research Center Neurosensory Science, Carl von Ossietzky University, Oldenburg, Germany

Abstract

Axons from the nucleus magnocellularis (NM) and their targets in nucleus laminaris (NL) form the circuit responsible for encoding interaural time differences. In barn owls, NL receives bilateral inputs from NM such that axons from the ipsilateral NM enter NL dorsally, while contralateral axons enter from the ventral side. These afferents and their synapses on NL neurons generate a tone-induced local field potential, or neurophonic, that varies systematically with position in NL. From dorsal to ventral within the nucleus, the best interaural time difference (ITD) of the neurophonic shifts from contralateral space to best ITDs around 0 μ s. Earlier recordings suggested that in NL, iso-delay contours ran parallel to the dorsal and ventral borders of NL (Sullivan and Konishi, 1986). This axis is orthogonal to that seen in chicken NL, where a single map of ITD runs from around 0 μ s ITD medially to contralateral space laterally (Köppl and Carr, 2008). Yet the trajectories of the NM axons are similar in owl and chicken (Seidl and Grothe, 2005). We therefore used clicks to measure conduction time in NL, and made lesions to mark the 0 μ s iso-delay contour in multiple penetrations along an iso-frequency slab. Iso-delay contours were not parallel to the dorsal and ventral borders of NL; instead the 0 μ s iso-delay contour shifted systematically from a dorsal position in medial NL to a ventral position in lateral NL. Could different conduction delays

account for the mediolateral shift in the representation of 0 μ s ITD? We measured conduction delays using the neurophonic potential, and developed a simple linear model of the delay line conduction velocity. We then raised young owls with time-delaying ear plugs in one ear (Gold and Knudsen, 1999) to examine map plasticity.

Keywords

sound localisation; phase locking; ITD; barn owl; plasticity

1. Introduction

The barn owl's nucleus laminaris remains an outstanding preparation for analysing ITD coding. A major advantage is its large size and accessibility. The nuclei of the auditory brainstem occupy most of the floor of the fourth ventricle, allowing for precise mapping of ITDs *in vivo*. NL also is a useful preparation for the experimental manipulation of developmental events, because the barn owl's head size more than doubles in size during the first month posthatch (Köppl et al., 2005). We have therefore used the neurophonic potential to measure the conduction times needed to create maps of ITD, and developed a simple linear model of the delay line conduction velocity.

Neurophonics are extracellular potentials well correlated with auditory stimuli, and are found in mammals and birds (Köppl and Carr, 2008; Sullivan and Konishi, 1986; McLaughlin et al., 2010; Schwarz, 1992; Köppl and Carr, 2008; Sullivan and Konishi, 1986). Although its precise source(s) are still uncertain and may differ between species (Köppl et al., 2008; McLaughlin et al., 2009; Schwarz, 1992) the neurophonic is generally accepted as a valid reflection of local activity within the NL.

2. Materials and Methods

The experiments were conducted at the Departments of Biology of the University Maryland and University of Oldenburg. 18 barn owls (*Tyto alba*) were used to collect the data presented in this and other studies (Wagner et al., 2005; 2009; Kuokkanen et al., 2010). Procedures conformed to NIH guidelines for Animal Research and were approved by the Animal Care and Use Committee of the Universities of Maryland and Oldenburg. Anaesthesia was induced by intramuscular injections of 10–20 mg/kg ketamine hydrochloride and 3–4 mg/kg xylazine. Supplementary doses were administered to maintain a suitable plane of anaesthesia. Body temperature was maintained at 39°C by a feedback-controlled heating blanket. For mapping experiments, electrodes were moved in defined amounts in the rostrocaudal and mediolateral axes. More details may be found in Wagner et al., (2009).

Recordings were made in a sound-attenuating chamber (IAC, New York). Tungsten electrodes were used, with impedances between 5 and 20 M Ω . A grounded silver chloride pellet, placed under the animal's skin around the incision, served as the reference electrode. Amplified electrode signals were passed to a threshold discriminator (SD1 (Tucker-Davis Technologies (TDT) Gainesville, FL)) and an analogue-to-digital converter (DD1 (TDT))

connected to a personal computer via an optical interface (OI (TDT)). Acoustic stimuli were digitally generated by custom-written software ("Xdphys" written in Dr. M. Konishi's lab at Caltech) driving a signal-processing board (DSP2 (TDT)). Acoustic signals were fed to miniature earphones, inserted into the owl's left and right ear canals, respectively. At a given recording site, we measured frequency tuning, then tuning to interaural time difference, and responses to monaural clicks. For most penetrations, an electrolytic lesion (1–10 μ A, 3–10sec) was made at or near the response to best ITD of 0 μ s. After a survival time of 5–14 days, owls were perfused transcardially with saline, followed by 4% paraformaldehyde in phosphate buffer. Brains were blocked in the same stereotaxic apparatus as for in vivo recordings, and sections through NL were reconstructed with the aid of a NeuroLucida system.

Young owls were raised from about posthatching day 20 with earplugs designed by Gold and Knudsen to introduce a time delay in the 3–5 kHz inputs from one ear (Gold and Knudsen, 1999). Maps of ITD were investigated as above in owls raised with earplugs, and lesions made as above.

3. Results

NL receives bilateral inputs from the nucleus magnocellularis (NM) such that axons from the ipsilateral NM enter NL dorsally, while contralateral axons enter from the ventral side. These afferents, and their synapses on NL neurons, generate the neurophonic, which varies systematically with position in NL (Figure 1; Kuokkanen et al., 2010; Sullivan and Konishi, 1986; Kuokkanen et al., 2010). From dorsal to ventral within NL, the best ITD of the neurophonic shifts from contralateral space to best ITDs around 0 μ s, and on to ipsilateral ITDs. Neurophonics were used to map best ITD, accompanied by small electrolytic lesions, generally at the location of the response to 0 μ s ITD. Based on our 3D reconstructions of NL architecture and our measures of delay, we generated an explanation of how conduction velocity of the incoming delay-lines axons from NM creates these maps, and used modelling to constrain measurements of conduction velocity.

3.1 Dorsoventral Maps of ITD in Owls

Within NL, binaurally evoked neurophonics vary with interaural phase difference, as do ITD-sensitive responses recorded from NL neurons (Carr and Konishi, 1990; Pena et al., 2001). The maximum neurophonic response to best IPD changes systematically with depth, always shifting towards ipsilateral space (Sullivan and Konishi, 1986); Fig 2A). These location-dependent shifts in best IPD only occur within NL; lesions marking the onset of the systematic shift are found on the dorsal edge of the nucleus, and those marking the end of the phase shift are on the ventral edge (Sullivan and Konishi, 1986).

We measured the changes in the neurophonic obtained when traversing the short, dorsoventral axis of NL. From dorsal to ventral within NL, the phase delay of a contralaterally elicited potential decreased and that of its ipsilateral counterpart increased (Sullivan and Konishi, 1986). This neurophonic delay reflects the delay of phase-locked spikes originating from interdigitating ipsi- and contralateral axons from NM, and generates an orderly representation of delay disparities. NL is tonotopically organized, and its

isofrequency laminae are oriented along a plane that is inclined about 45° to the midline. We quantified the distribution of ITDs within a single isofrequency lamina by stereotactically sampling ITD at multiple locations along this diagonal. Each isofrequency lamina contained a map of optimal binaural delays. The map is best illustrated by iso-delay contours (Fig. 2B).

Medial portions of each tonotopic lamina mapped best ITDs near 0 μ s dorsally in NL, with a representation of ipsilateral space below (Fig. 2B). The central portions of the tonotopic lamina contained maps of best ITD that were centred on frontal space. The most lateral lesions were characterized by representations of contralateral space, and the most extreme lateral positions did not include a representation of 0 μ s. Thus there was a steady shift in the mapping of 0 μ s from dorsal in medial NL to ventral in lateral NL.

3.2 ITD at 0 can be Derived from Latencies of Click-induced responses

Since the representation of frontal space shifted systematically to more ventral locations with mediolateral progression along each tonotopic band, we measured delay latency at different mediolateral positions to determine the basis of the shift and to show how regulation of conduction velocity could underlie map formation. Click stimuli provide a useful measure of conduction delay, since click phase is precise (Wagner et al., 2005). We compared the neurophonic responses to ipsi- and contralateral clicks at best ITDs at or near 0 μ s, and observed overlaid, phase-locked but not identical ipsi- and contralateral click responses (Fig. 3A).

3.3 Models of Conduction Velocity and Maps of ITD

We developed a simple linear model of NL that incorporated click delays (Fig. 3B). Conduction velocities along the delay lines inside (d_1 – d_4) and outside NL (l_1 – l_4) were assumed to be different but constant, consistent with our measures of axon diameter and intermodal distance (Carr and Konishi, 1990; Carr and Boudreau, 1993). Also, we assumed a common path from NM to the midline, followed by a measured path from the midline to the edges of NL. Axon lengths were estimated using a predefined straight-line geometry, derived from reconstructions of axon paths. The parameters of this geometry were fit to three-dimensional reconstructions of the NL borders and the locations of lesions reconstructed from counterstained sections.

The model was used to evaluate possible conduction velocities along the delay lines in NL. The model yielded a range of possible conduction velocities lying between 1 and 10 m/s with velocities within the nucleus being smaller than those outside NL. The model also showed that iso-ITD lines running parallel to the dorsal and ventral borders of NL in the medio-lateral direction (Sullivan and Konishi, 1986) yielded biologically unrealistic conduction velocities, thus predicting the experimentally observed iso-ITD contours.

3.4 Plasticity in Maps of ITD

Young owls (from P21) were unilaterally fitted with an ear-canal insert designed to introduce a time delay to inputs from that ear (Gold and Knudsen, 1999, *J. Neurophysiol.* 5: 2197–2209). After growing up with this altered auditory experience, the representation of ITD in

NL was mapped using neurophonic responses and tested for any differences to normal. Our hypothesis was that, if NL adjusts for the temporally altered input, the maps of ITD would be shifted compared to normal. In addition, complementary shifts are expected in the NL of both sides. Specifically, on the side ipsilateral to the ear insert, the point of zero ITD should shift ventrally, and dorsally on the contralateral side. Preliminary analysis did not reveal any shifts in the predicted, adaptive direction. This suggests that nucleus laminaris does not show experience-dependent plasticity, at least not after P20–30. The data are consistent with the observation that myelination of the delay lines peaks at the third week post hatch (Cheng and Carr, 2007)..

4. Discussion

Based on NL architecture and our results, we have generated an explanation of how conduction velocity of the incoming delay lines axons from NM create these maps, and used models to constrain measurements of conduction velocity.

4.1 Models of Conduction Velocity and Maps of ITD

In the barn owl and chicken, the bilateral projection from NM to NL conforms to the requirements of the Jeffress model. In the barn owl, NM axons innervate dorso-ventral arrays of neurons in NL in a sequential fashion. For each frequency band, recordings from these interdigitating ipsilateral and contralateral axons show regular changes in delay with depth in NL (Carr and Konishi, 1990). These conduction delays are similar to the $\pm 250\mu\text{s}$ range of ITDs available to the barn owl (Campenhausen and Wagner, 2006).

The delay line circuit in the chicken is organized on the same plan as the circuit described for the barn owl, except that NL is not a large nucleus, but a monolayer of bipolar cells oriented in the medio-lateral dimension of the brainstem (Parks and Rubel, 1975; Young and Rubel, 1983; Seidl et al., 2010). NL cells receive input from the ipsilateral NM, which splay out to innervate NL neurons with approximately equal lengths to each cell, so that ipsilateral inputs arrive fairly simultaneously along the medio-lateral extent of NL. The contralateral axons act as delay lines; each axon runs along the ventral surface of NL, giving off collateral branches in the nucleus. Patterns of axons in the cat MSO are very similar to those of the chicken, in that axons from the contralateral ventral cochlear nucleus project across the rostro-caudal axis of the nucleus, while the ipsilateral axons form a less organized projection (Smith et al., 1993; Beckius et al., 1999). The advantage of birds is that NL is fairly straight and delays can therefore be mapped within a single tonotopic band. We therefore were able to measure delays with precision, to determine how continuous maps of IPD are formed, and found that the three-dimensional network of delays representing response latencies is well suited for the derivation of interaural phase differences by coincidence detection, with long delays in the dorsoventral dimension and short delays in the mediolateral dimension.

Acknowledgments

This research was sponsored by NIH DC00436 to CEC, by NIH P30 DC04664 to the University of Maryland Center for the Comparative and Evolutionary Biology of Hearing, by the German Research Foundation (DFG, Wa-606/12, Ke-788/1-3, 4), by the Bundesministerium für Bildung und Forschung (BMBF, Bernstein Collaboration

Temporal Precision, 01GQ07101 to HW and 01GQ07102 to RK), and by fellowships from the Humboldt foundation and the Hanse Wissenschaftskolleg to CEC and GA.

References

- Beckius GE, Batra R, Oliver DL. Axons from anteroventral cochlear nucleus that terminate in medial superior olive of cat: observations related to delay lines. *J. Neurosci.* 1999; 19:3146–3161. [PubMed: 10191328]
- Campeaux M, Wagner H. Influence of the facial ruff on the sound-receiving characteristics of the barn owl's ears. *J. Comp. Psychol.* 2006; 192:1073–1082.
- Carr CE, Boudreau RE. Organization of the nucleus magnocellularis and the nucleus laminaris in the barn owl: encoding and measuring interaural time differences. *J. Comp. Neurol.* 1993; 334:337–355. [PubMed: 8376623]
- Carr CE, Konishi M. A circuit for detection of interaural time differences in the brain stem of the barn owl. *J. Neurosci.* 1990; 10:3227–3246. [PubMed: 2213141]
- Gold JI, Knudsen EI. Hearing impairment induces frequency-specific adjustments in auditory spatial tuning in the optic tectum of young owls. *J. Neurophys.* 1999; 82:2197–2209.
- Köpl C, Carr CE. Maps of interaural time difference in the chicken's brainstem nucleus laminaris. *Biol. Cyber.* 2008; 98:541–559.
- Köpl C, Futterer E, Nieder B, Siermann R, Wagner H. Embryonic and posthatching development of the barn owl (*Tyto alba*): reference data for age determination. *Dev. Dyn.* 2005; 233:1248–1260. [PubMed: 15861405]
- Kuokkanen PT, Wagner H, Ashida G, Carr CE, Kempter R. On the origin of the extracellular field potential in the nucleus laminaris of the barn owl (*Tyto alba*). *J. Neurophys.* 2010; 104:2274–2290.
- McLaughlin M, Verschooten E, Joris PX. Oscillatory dipoles as a source of phase shifts in field potentials in the mammalian auditory brainstem. *J. Neurosci.* 2010; 30:13472–13487. [PubMed: 20926673]
- Parks TN, Rubel EW. Organization and development of brain stem auditory nuclei of the chicken: organization of projections from n. magnocellularis to n. laminaris. *J. Comp. Neurol.* 1975; 164:435–448. [PubMed: 1206128]
- Pena JL, Viète S, Funabiki K, Saberi K, Konishi M. Cochlear and Neural Delays for Coincidence Detection in Owls. *J. Neurosci.* 2001; 21:9455–9459. [PubMed: 11717379]
- Schwarz DW. Can central neurons reproduce sound waveforms? An analysis of the neurophonic potential in the laminar nucleus of the chicken. *The Journal of Otolaryngol.* 1992; 21:30–38.
- Seidl A, Grothe B. Development of Sound Localization Mechanisms in the Mongolian Gerbil Is Shaped by Early Acoustic Experience. *J. Neurophys.* 2005; 94:1028–1036.
- Seidl AH, Rubel EW, Harris DM. Mechanisms for adjusting interaural time differences to achieve binaural coincidence detection. *J. Neurosci.* 2010; 30:70–80. [PubMed: 20053889]
- Smith PH, Joris PX, Yin TCT. Projections of physiologically characterized spherical bushy cell axons from the cochlear nucleus of the cat: evidence for delay lines to the medial superior olive. *J. Comp. Neurol.* 1993; 331:245–260. [PubMed: 8509501]
- Sullivan WE, Konishi M. Neural map of interaural phase difference in the owl's brainstem. *Proc. Natl. Acad. Sci. USA.* 1986; 83:8400–8404. [PubMed: 3022292]
- Wagner H, Brill S, Kempter R, Carr CE. Microsecond precision of phase delay in the auditory system of the barn owl. *J. Neurophys.* 2005; 94:1655–1658.
- Wagner H, Brill S, Kempter R, Carr CE. Auditory responses in the barn owl's nucleus laminaris to clicks: impulse response and signal analysis of neurophonic potential. *J. Neurophys.* 2009; 102:1227–1240.
- Young S, Rubel EW. Frequency-specific projections of individual neurons in chick brainstem auditory nuclei. *J. Neurosci.* 1983; 3:1373–1378. [PubMed: 6864252]

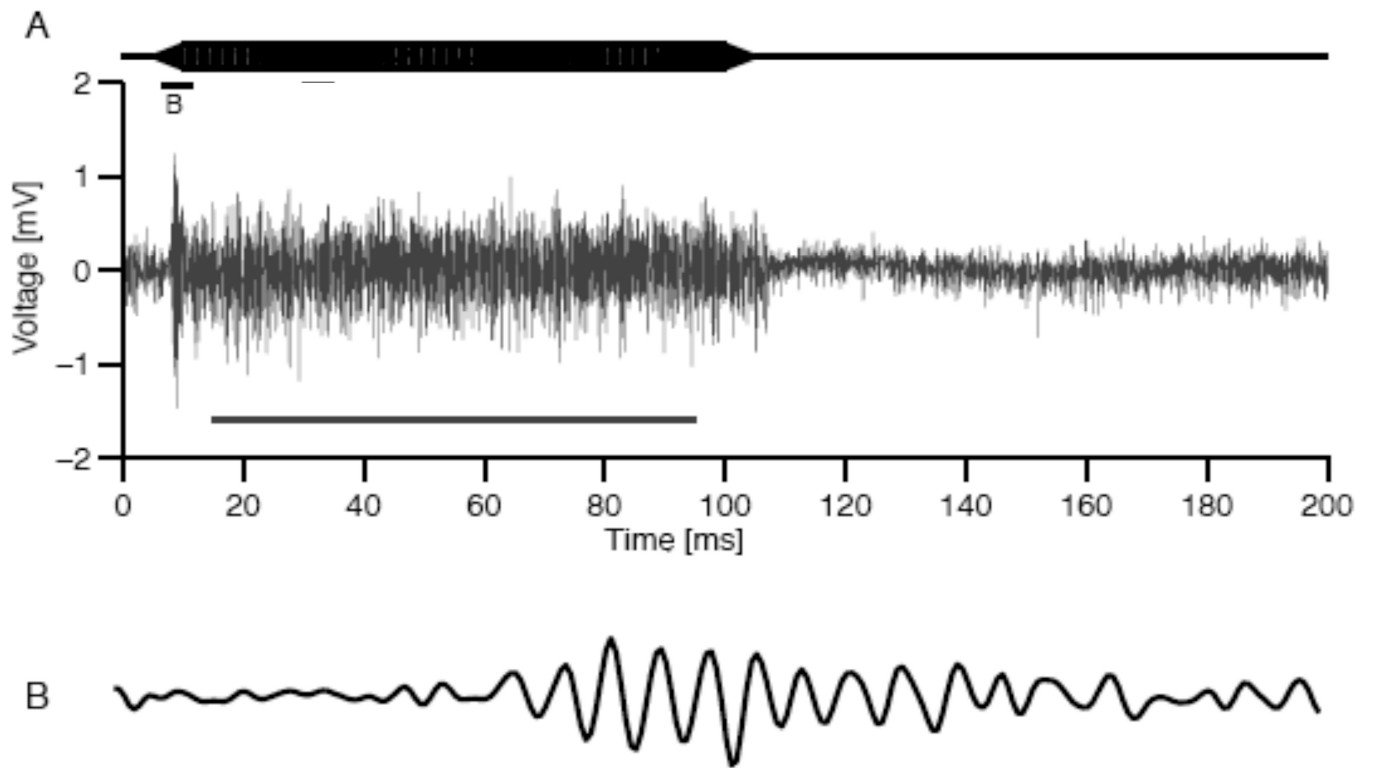


Fig. 1.
A. 5kHz tone stimulus (top) and neurophonic response (bottom). B. 5ms interval of the neurophonic at tone onset. Modified from Kuokkanen et al., 2010.

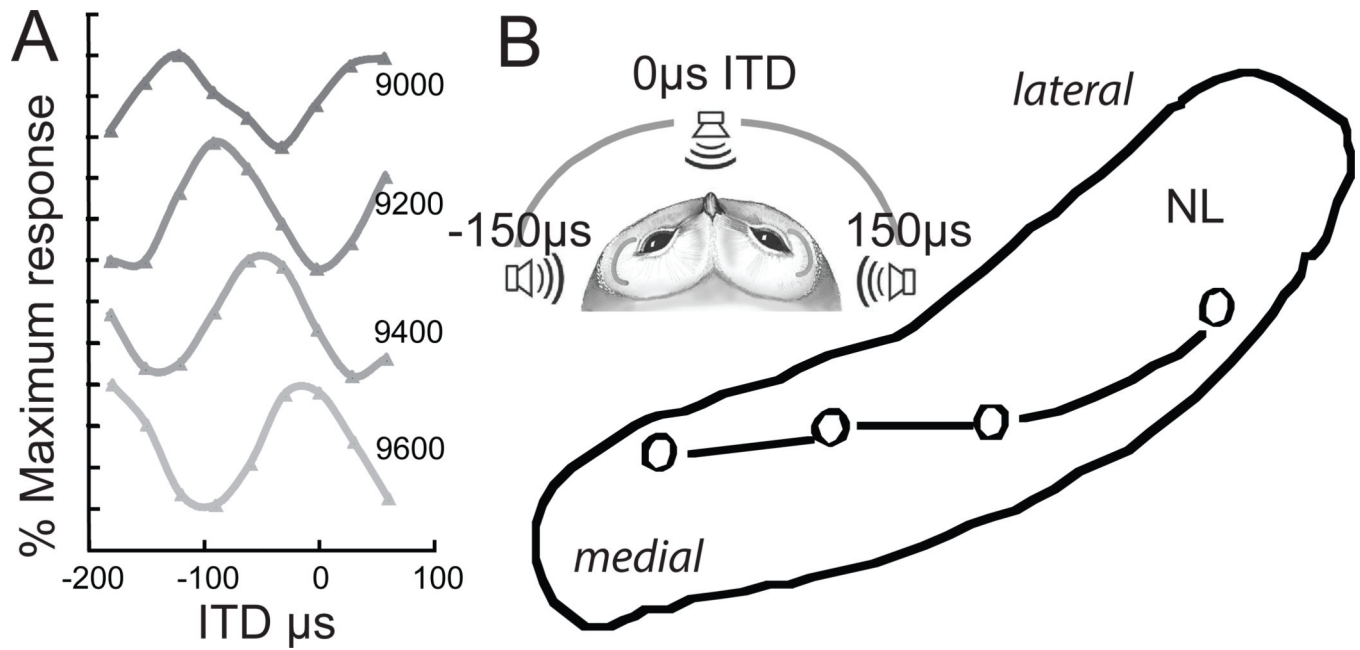


Figure 2.

A. Neurophonic responses recorded at 200 μm intervals in a single penetration through NL.

B. Lesions were placed at 0 μs ITDs in multiple penetrations through NL, revealing iso-ITD lines were not parallel to the borders of NL. Insert: Schematic owl head showing range of ITDs (Campenhausen and Wagner, 2006).

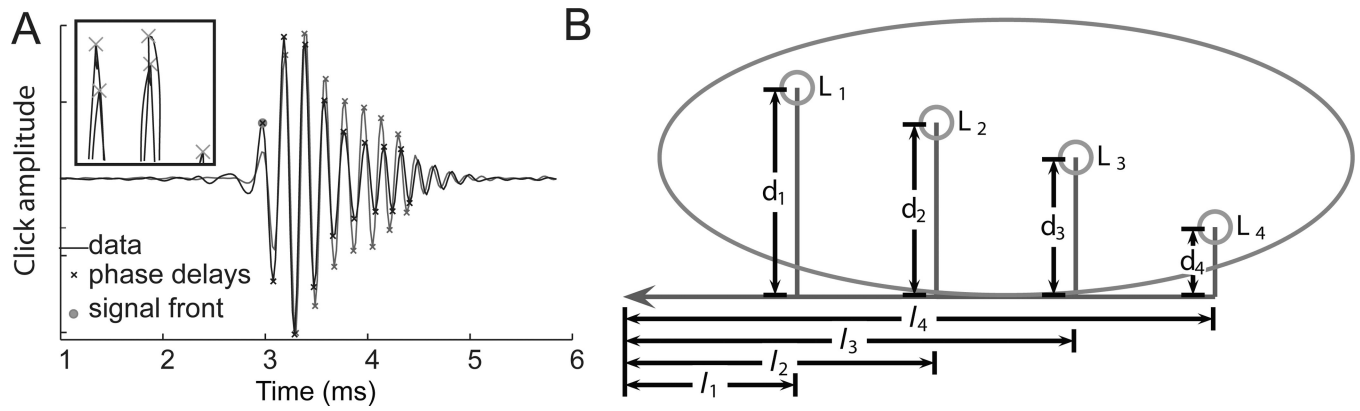


Figure 3. A. Left and right neurophonic clicks responses recorded at $0\mu\text{s}$ best ITD. B. Model of neurophonic conduction velocity accounts for observed shifts in best ITD.